



HAL
open science

1 to 220 GHz complex permittivity behavior of flexible polydimethylsiloxane substrate

Pierre-Yves Cresson, Yovan Orlic, Jean-François Legier, Erick Paleczny, Luc Dubois, Nicolas Tiercelin, Philippe Coquet, Philippe Pernod, Tuami Lasri

► **To cite this version:**

Pierre-Yves Cresson, Yovan Orlic, Jean-François Legier, Erick Paleczny, Luc Dubois, et al.. 1 to 220 GHz complex permittivity behavior of flexible polydimethylsiloxane substrate. *IEEE Microwave and Wireless Components Letters*, 2014, 24 (4), pp.278-280. 10.1109/LMWC.2013.2295230 . hal-00980037

HAL Id: hal-00980037

<https://hal.science/hal-00980037>

Submitted on 20 Oct 2020

HAL is a multi-disciplinary open access archive for the deposit and dissemination of scientific research documents, whether they are published or not. The documents may come from teaching and research institutions in France or abroad, or from public or private research centers.

L'archive ouverte pluridisciplinaire **HAL**, est destinée au dépôt et à la diffusion de documents scientifiques de niveau recherche, publiés ou non, émanant des établissements d'enseignement et de recherche français ou étrangers, des laboratoires publics ou privés.

1 to 220 GHz Complex Permittivity Behavior of Flexible PDMS (Polydimethylsiloxane) Substrate

P.-Y. Cresson¹ ; Y. Orlic²; J.-F. Legier¹ ; E. Paleczny¹ ; L. Dubois¹ ; N. Tiercelin² ; P. Coquet²; P. Pernod² ; T. Lasri¹

1- Institut d'Electronique, de Microélectronique et de Nanotechnologie (IEMN-UMR 8520), MITEC group, University of Lille 1, Villeneuve d'Ascq 59652, France

2- Joint International Laboratory LIA LEMAC/LICS: IEMN, UMR CNRS 8520, PRES University of Lille Nord de France, EC Lille and the University of Lille1, Villeneuve d'Ascq 59651, France

Abstract:

Coplanar transmission lines (CPW) are realized on polydimethylsiloxane (PDMS) substrate in order to characterize its complex permittivity, from 1 to 220 GHz. By varying the complex permittivity, the propagation constant of the PDMS-CPW calculated with full wave software is matched to those extracted by de-embedding techniques using S-parameters measurements. The real permittivity evolves from 2.9 to 2.55 while the loss tangent increases slowly to reach 0.048 at 210 GHz.

Published in: [IEEE Microwave and Wireless Components Letters](#) (Volume: 24 , Issue: 4 , April 2014) Page(s): 278 - 280

I. Introduction

During the past decade, the continuous efforts in studying chemistry, mechanics, organic LED and transfer printing process provided innovative ways for low frequency flexible electronic applications based on polymers [1]. These foldable polymers substrates are very promising for mm-wave band applications that are in full expansion. Among these polymers, PDMS has recently gained much attention for the development of μ -wave and mm-wave tunable antennas [2], [3], tunable phase shifters [4], and RF switch [5]. Indeed PDMS exhibits attractive features: it is low cost, light weight, easy to process and extremely flexible with a very low Young's modulus ($E_{\text{Young}}=2$ MPa). To give realistic predictions of characteristic impedance and overall losses of such planar structures, the knowledge of the polymer dielectric properties is essential [6]. To that end, we present in this letter the dielectric characterization of PDMS from 1 GHz up to 220 GHz, which to the authors knowledge has not been done before. This is achieved thanks to coplanar transmission lines (PDMS-CPW) realization for the complex propagation constant extraction from S-parameters measurements that are used for the matching with two full-wave software.

II. Fabrication of CPW Lines and Sizing

Patterning conductive lines on PDMS can be difficult due to the polymer high thermal expansion coefficient. To ensure a good precision, the lines are patterned on a sacrificial layer using classical microfabrication methods and then reported on PDMS. The fabrication process is derived from [7] and is described in Fig. 1.

First a 100 nm molybdenum (Mo) sacrificial layer is sputtered on a silicon wafer. After photolithography, a 500 nm gold layer is sputtered, and then followed by the deposition of the adhesion layer: 50 nm of sputtered titanium topped by 50 nm of PECVD silicon oxide. Then, a thick PDMS film ($\approx 180 \mu\text{m}$) is deposited by spin coating. This procedure ends with the etching of the Mo layer and the PDMS sample to be characterized is released. The polymer material used here is a Dow Corning's Sylgard 184 silicon elastomer.

A SEM image of one of the fabricated PDMS-CPW is given in Fig. 2. One can see the footprint left by the probes used for the experimental characterization.

To maintain the single-mode behavior up to 300 GHz, the PDMS-CPW (Fig. 3) must be properly designed. For this purpose, the transverse dimensions of the CPW (Table I), are chosen considering a compromise between substrate thickness H , ground to ground spacing $(W+2S)$ and total width $(2W_g+W+2S)$ which predetermine the occurrence of higher order modes [8].

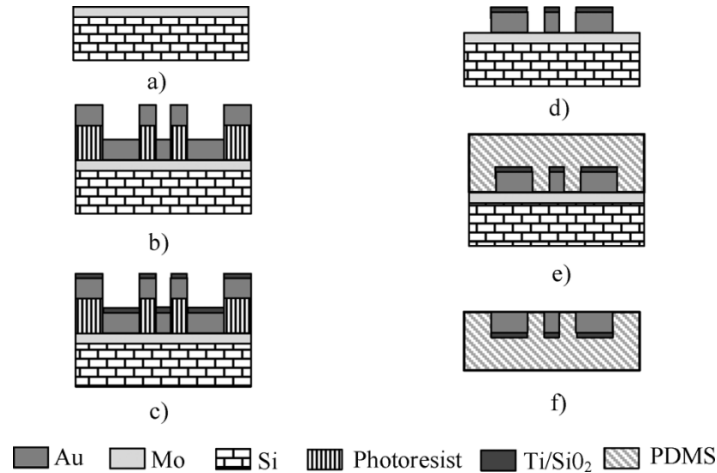


Fig. 1. Fabrication process for CPW lines printed on PDMS substrate. (a) Molybdenum sputtering. (b) Au sputtering. (c) Adhesion layer deposition. (d) Lift off. (e) PDMS spin coating. (f) Molybdenum etching and release.

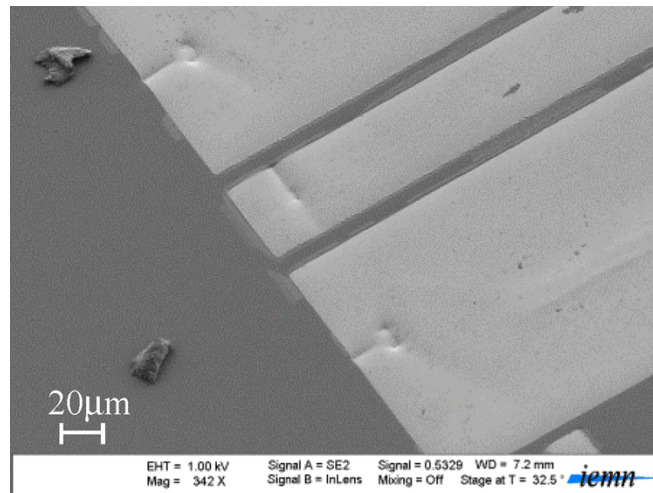


Fig. 2. SEM photograph of a PDMS-CPW.

Table I: Geometrical Parameters of the PDMS-CPW Lines

	W_g (μm)	S (μm)	W (μm)	Z_o (Ω)	L (mm)
Lines A	150	15	45	76	3 / 5 / 10
Lines B	200	10	70	66	3 / 5 / 10

We have fabricated ten lines of each type (A and B) with 3, 5, or 10 mm length. For the 2 types of lines, the characteristic impedance Z_o was calculated using the complex permittivity of PDMS proposed in [7]. A thickness of $t=0.43 \mu\text{m}$ for the gold strip conductors of mean value of conductivity $\sigma=3.37 \cdot 10^7 \text{ S/m}$ has been measured during the technological process as well as the PDMS substrate height $H=182 \mu\text{m}$.

III. Measurement Protocols and Setup

Our protocol relies first, on the determination of the complex propagation constant $\gamma=\alpha+j\beta$ extracted from on-wafer S-parameters measurements of PDMS-CPW having the same impedance [9], [10]. In the finite element (FEM) protocol, the resulting data for γ are inputs of an inversion algorithm. It makes use of commercial MATLAB® (R2010a) root-searching algorithm and FEM from COMSOL® software (v4.1). The role of FEM is to predict the propagation constant of the PDMS-CPW which is matched to the measured ones by iterative refinement of the real permittivity (ϵ_r) and loss tangent ($\tan\delta$) values, for each frequency point. The FEM protocol allows to separate out, very accurately, the dielectric losses from the metallic ones because it takes into account the metallization of finite conductivity and of finite thickness, by meshing inside the conductor. As the FEM is very time consuming for the calculation and requires a large size of memory, we have also developed a second protocol where the spectral domain approach (SDA) replaces the FEM. SDA makes use of an integral equations development applied in the spectral domain, and is coupled with a method of moment. We have initially developed the software to provide the propagation constant of any transmission line [11]. But for the present needs, it has been modified to obtain directly the real permittivity and the loss tangent which are the zero of a complex function. This is done without any iterative procedure.

Concerning the S-parameters measurements, they are carried out on two broadband systems, consisting of a 8510c HP vector network analyzer (VNA) for the 0.045 to 110 GHz frequency band and of a Rohde&Schwarz ZVA 24 coupled to an extension module V05 VNA-T/R/X2 supplied by OML company for the 140–220 GHz range. They are respectively connected to a cascade summit 11 K and Suss microtech PM8 probe station. The pitch of the G-S-G probe for the two systems is 100 μm .

IV. Measurements Results and Discussion

After calibration using LRRM method at room temperature, we can observe, for two lines (type A and B) as a typical example, the behavior of the complex propagation constant extracted from the de-embedding of S-parameters (Fig. 4). We note that at 30 and 200 GHz, the magnitude of the phase constant, for the two CPW lines, is approximately twenty and forty times greater than the magnitude of the attenuation constant. The linearity of the phase constant with respect to the frequency deviates by less than 2% compared to the theoretical case of a plane wave with a slope of 28.37 rad/m per GHz. This gives, for example, relative effective dielectric permittivity values of 1.909, 1.836, and 1.843 at 30, 100, and 200 GHz, respectively. This quantitative appraisal shows that the CPW mode is quasi-TEM with reasonable losses.

Figs. 5 and 6 exhibit the real permittivity and loss tangent behaviors of PDMS. We have selected among the data concerning the set of CPW lines, those which give the maximum and minimum values obtained with FEM protocol. The mean values curve corresponds to the averaging over the whole results. The grey squares represent the values obtained by the SDA applied to the average value of the attenuation and phase constant. It can be seen that the agreement between the results obtained with the two methods is very good.

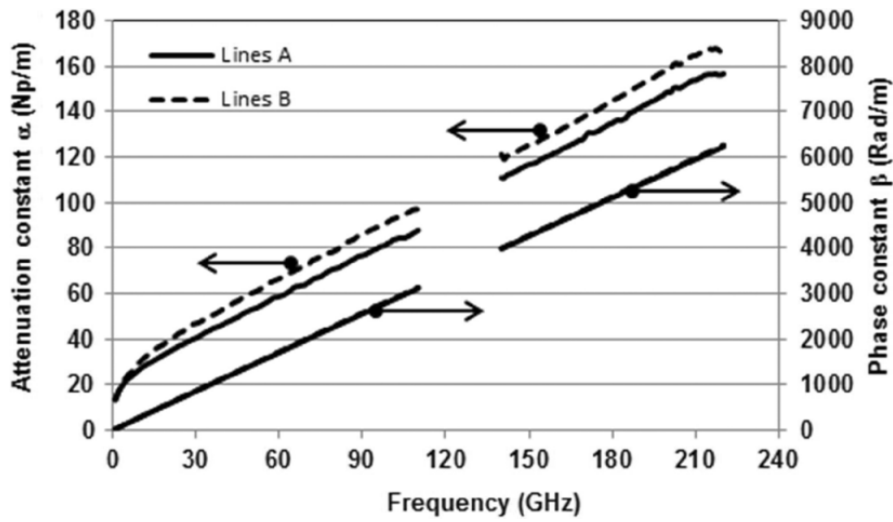


Fig. 4. Attenuation and phase constant measured in a frequency band of 1 to 220 GHz for PDMS-CPW.

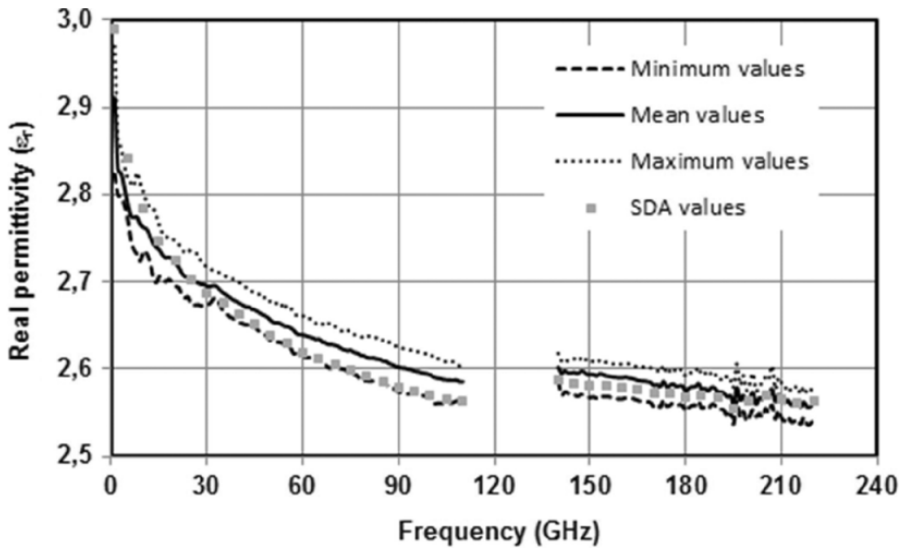


Fig. 5. Real permittivity, ϵ_r , in a band of 1 to 220 GHz for PDMS.

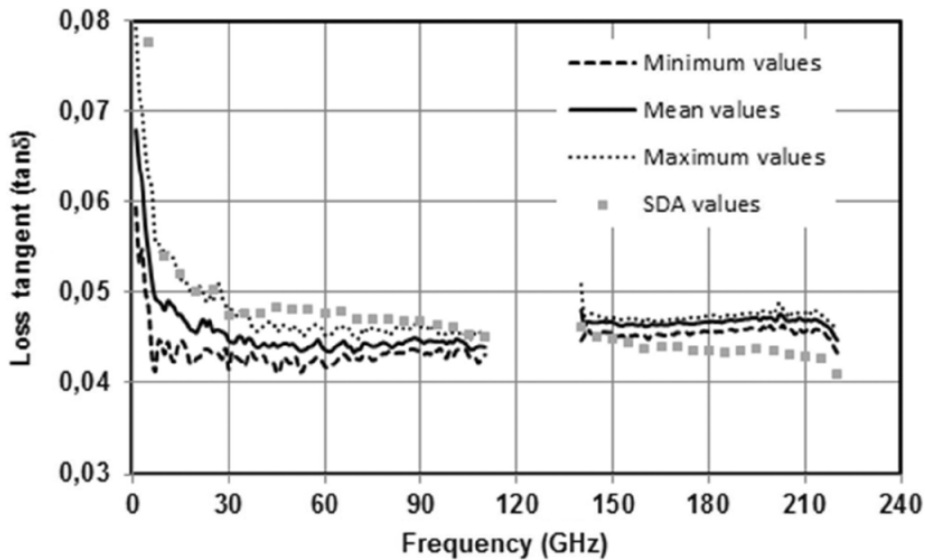


Fig. 6. Loss tangent, $\tan\delta$, in a band of 1 to 220 GHz for PDMS.

Figs. 7 and 8 show the standard deviation and the relative dispersion (three times the standard deviation divided by the mean value). The standard deviation magnitude is very low, indicating

good repeatability for measurements of the complex permittivity, but with a degradation between 1 to 30 GHz for the loss tangent. This effect is linked to the contribution of dielectric losses to the whole attenuation. The attenuation due to dielectric losses tends to zero as the frequency goes to zero.

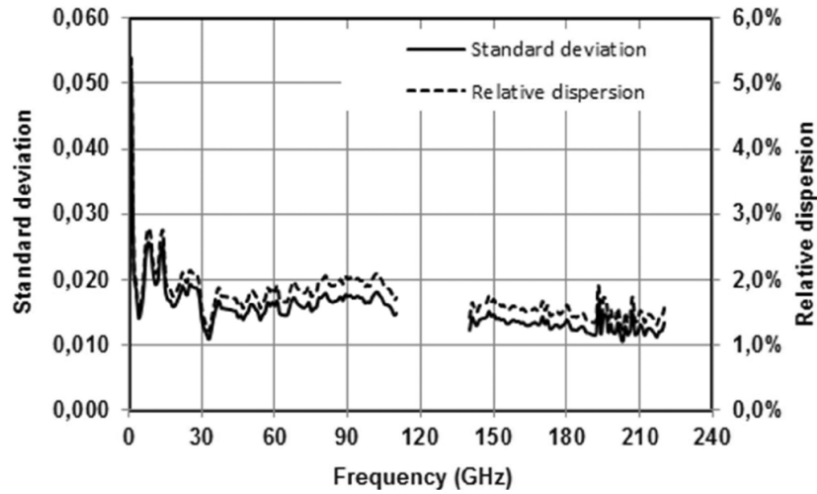


Fig. 7. Standard deviation and relative dispersion for ϵ_r measurement.

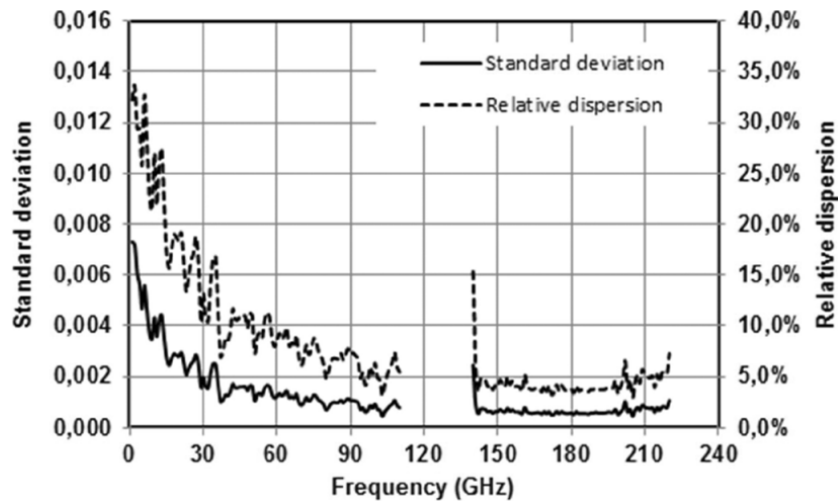


Fig. 8. Standard deviation and relative dispersion for $\tan\delta$ measurement.

Table II: Comparison of Dielectric Properties for PDMS (*: This Work)

Frequency	5 GHz	40 GHz	77 GHz
ϵ_r	2.77* / 2.8 [6]	2.68* / 2.75 [6]	2.62* / 2.67 [7]
$\tan\delta$	0.054* / 0.016 [6]	0.044* / 0.045 [6]	0.044* / 0.04 [7]

The relative discrepancies do not exceed 3% except for the lowest frequencies (1 GHz, 7%). These data match well despite the fact that they use radically different measurement methods. The same holds for the loss tangent with reasonable disparities (<15%) except below 30 GHz where the dielectric losses become more and more noisy as the frequency decreases. Table II compares our results with published ones at 3 frequencies. A good agreement is observed except for the lowest frequency.

V. Conclusion

We present in this letter the dielectric characterization of PDMS, up to 220 GHz. The complex permittivity is calculated with FEM and SDA methods from S-parameters measurements on CPW lines. The analysis of the experimental results, based on the FEM reference protocol, exhibits typical values of 2.91 (0.068), 2.75 (0.048), 2.59 (0.0445) and 2.57 (0.048) at 1, 10, 100, and 200 GHz for ϵ_r and $\tan\delta$ (in brackets) respectively. The major interest of the SDA lies in the speed of computing solutions (50 times faster than FEM) that allows real time knowledge of PDMS dielectric parameters with good confidence. All these results together show the efficiency and the reliability of the characterization methods developed.

Acknowledgements

The authors thank Ms. S. Lepilliet and Ms. V. Avramovic for helping them with the S-parameters measurements.

References

- [1] J. A. Rogers, T. Someya, and Y. Huang, "Materials and mechanics for stretchable electronics," *Science*, vol. 327, pp. 1603–1606, Mar. 2010.
- [2] J.-H. So, J. Thelen, A. Qusba, G. J. Hayes, G. Lazzi, and M. D. Dickey, "Reversibly deformable and mechanically tunable fluidic antennas," *Adv. Functional Mater.*, vol. 19, pp. 3632–3637, Nov. 2009.
- [3] S. Hage-Ali, N. Tiercelin, P. Coquet, R. Sauleau, V. Preobrazhensky, and P. Pernod, "A millimeter-wave in flatable frequency agile elastomeric antenna," *IEEE Antennas Wireless Propag. Lett.*, vol. 9, pp. 1131–1134, 2010.
- [4] S. Hage-Ali, Y. Orlic, N. Tiercelin, R. Sauleau, P. Pernod, V. Preobrazhenski, and P. Coquet, "A millimeter-wave elastomeric microstripphase shifter," in *IEEE MTT-S Int. Dig.*, Montréal, QC, Canada, Jun. 17–22, 2012, pp. 1–3.
- [5] C. M. Shah, S. Sriram, M. Bhaskaran, M. Nasabi, T. G. Nguyen, W. S. T. Rowe, and A. Mitchell, "Elastomer-based pneumatic switch for radio frequency microdevices," *J. Microelectromech. Syst.*, vol. 21, no. 6, pp. 1410–1417, Dec. 2012.
- [6] N. J. Farcich, J. Salonen, and P. M. Asbeck, "Single-length method used to determine the dielectric constant of polydimethylsiloxane," *IEEE Trans. Microw. Theory Tech.*, vol. 56, no. 12, pp. 2963–2971, Dec. 2008.
- [7] N. Tiercelin, P. Coquet, R. Sauleau, V. Senez, and H. Fujita, "Polydimethylsiloxane membranes for millimeter-wave planar ultra-flexible antennas," *J. Micromech. Microeng.*, vol. 16, pp. 2389–2395, Nov. 2006.
- [8] F. Schneider, T. Tischler, and W. Heinrich, "Modeling dispersion and radiation characteristics of conductor-backed CPW with finite ground width," *IEEE Trans. Microw. Theory Tech.*, vol. 51, no. 1, pp. 137–143, Jan. 2003.
- [9] F. Ponchel, J. Midy, J. F. Legier, C. Soyer, D. Remiens, T. Lasri, and G. Gueguan, "Dielectric microwave characterization of (Ba,Sr)TiO₃ film deposited on high resistivity silicon substrate: Analysis by two-dimensional tangential finite element method", *J. Appl. Phys.*, vol. 107, no. 5, pp. 054112–054112-5, Mar. 2010.
- [10] J. Hinojosa, "S-parameter broadband measurements on-coplanar and fast extraction of the substrate intrinsic properties," *IEEE Microw. Wireless Compon. Lett.*, vol. 11, no. 2, pp. 80–82, Feb. 2001.
- [11] E. Paleczny, D. Kinowski, J. F. Legier, P. Pribetich, and P. Kennis, "Comparison of full wave approaches for determination of microstrip conductor losses for MMIC applications," *Electron. Lett.*, vol. 26, no. 90, pp. 2076–2077, Dec. 1990.